

Supporting Information

Step-by-step Mechanism Insights into TiO₂/Ce₂S₃ S-scheme Photocatalyst for Enhanced Aniline Production with Water as Proton Source

Feiyan Xu¹, Kai Meng², Shuang Cao², Chenhui Jiang³, Tao Chen³, Jingsan Xu^{4,} and Jiaguo Yu^{1,2,*}*

¹ Laboratory of Solar Fuel, Faculty of Materials Science and Chemistry, China University of Geosciences, 388 Lumo Road, Wuhan, 430074, P. R. China.

² State Key Laboratory of Advanced Technology for Materials Synthesis and Processing, Wuhan University of Technology, Wuhan 430070, P. R. China.

³ Hefei National Laboratory for Physical Sciences at Microscale, CAS Key Laboratory of Materials for Energy Conversion, Department of Materials Science and Engineering, University of Science and Technology of China, Hefei 230026, P. R. China.

⁴ School of Chemistry and Physics & Centre for Materials Science, Queensland University of Technology, Brisbane, QLD 4001, Australia.

*Correspondence: jingsan.xu@qut.edu.au (J.X.), yujiaguo93@cug.edu.cn (J.Y.)

1. Experimental Section

1.1 Synthesis of electrospun TiO₂ nanofibers

All the chemicals were of analytic grade. Poly(vinyl pyrrolidone) (PVP, MW=1300000) was purchased from Tianjin Bodi Chemical Co., Ltd and others were purchased from Shanghai Chemical Company. Typically, tetrabutyl titanate (TBT, 4.0 g) and PVP (1.5 g) were added into ethanol (20.0 g) and acetic acid (4.0 g) to form a transparent pale-yellow solution after magnetic stirring for several hours under room temperature. Then the solution was transferred into a 20 mL syringe in an electrospinning setup. The voltage, solution feeding rate and needle-to-collector distance of electrospinning were set to be 20 kV, 2.5 mL h⁻¹ and 10 cm, respectively. Afterwards, the collected TiO₂ precursor was annealed at 550 °C for 2 h with a heating rate of 2 °C min⁻¹ in air.

1.2 Preparation of TiO₂/Ce₂S₃ heterostructures

Typically, 0.03 mmol of Ce(NO₃)₃·6H₂O (equivalent to 1 mol% Ce₂S₃) and 0.06 mmol of hexamethylenetetramine were dissolved in 30 mL of water and 30 mL of ethanol to form a transparent solution. Then 1.5 mmol of TiO₂ nanofibers were added into the above solution to form a suspension. The suspension was transferred to a 100 mL Teflon-lined stainless steel autoclave and then heated in an oven at 75 °C for 12 h. The solid product was washed with deionized water and ethanol for three times and then dried at 60 °C in air. The obtained product was the TiO₂/CeO₂ precursor. For comparison, the precursor containing 0.5, 3, 5 and 7 mol% CeO₂ were also synthesized by varying the amounts of Ce(NO₃)₃·6H₂O and hexamethylenetetramine. To synthesize TiO₂/Ce₂S₃ heterostructures,

the TiO₂/CeO₂ precursors (~20 mg) were mixed with 0.1 g of thiocarbamide and calcined at 600 °C for 2 h at a heating rate of 10 °C min⁻¹ in Ar atmosphere. The obtained TiO₂/Ce₂S₃ heterostructures were labelled as TC_x, where T and C represent TiO₂ and Ce₂S₃, respectively; *x* is the mole percentage of Ce₂S₃ in TiO₂/Ce₂S₃ hybrids (*x* = 0.5, 1, 3, 5 and 7).

1.3 Characterization

XRD patterns were performed on a D/Max-RB X-ray diffractometer (Rigaku, Japan) with Cu *K*_α radiation. The morphology of samples was observed by a field emission scanning electron microscope (JSM 7500F, Japan). TEM images were recorded on a Titan G2 60-300 electron microscope equipped with an EDX spectrometer. UV-visible DRS was collected on a Shimadzu UV-2600 UV-visible spectrophotometer (Japan). XPS was carried out on a Thermo ESCALAB 250Xi instrument with Al *K*_α X-ray radiation. *In-situ* XPS was conducted under the same condition except that UV light irradiation was introduced. The steady-state PL emission spectra were collected on a Fluorescence Spectrophotometer (F-7000, Hitachi, Japan). TRPL spectra were recorded on a fluorescence lifetime spectrophotometer (FLS 1000, Edinburgh, UK) at an excitation wavelength of 375 nm. The *in-situ* FTIR analyses were carried out on Nicolet iS 50 spectrometer (Thermo fisher, USA) in two sequential steps. Initially, the photocatalyst was allowed to adsorb nitrobenzene and H₂O for 1 h in dark. The mixture of nitrobenzene and H₂O vapors were purged into the sample chamber with the continuous N₂ flow, which continuously passed through the solution containing nitrobenzene, H₂O and TEOA. Then, a 3 W-LED light of 365 nm was

turned on and illuminated for 2 h to *in-situ* monitor the photocatalytic hydrogenation of nitrobenzene. For CPD measurement, the samples were prepared by coating them on an ITO substrate and connected to the standard gold tip by the inner circuit. Electron paramagnetic resonance (EPR) was performed on an ESR spectrometer (MEX-nano, Bruker) with a modulation frequency of 100 kHz and a microwave power of 15 mW. Electrochemical measurements were conducted on an electrochemical analyzer (CHI660C, CH Instruments, Shanghai), in which Pt wire, Ag/AgCl (saturated KCl) and 0.5 M Na₂SO₄ solution functioned as counter electrode, reference electrode and electrolyte, respectively. Polarization curves were obtained by linear sweep voltammetry (LSV) with a scan rate of 5 mV s⁻¹. All applied potentials were converted with respect to reversible hydrogen electrode (RHE), namely, $E_{\text{RHE}} = E_{\text{Ag/AgCl}} + 0.059 \text{ pH} + 0.197 \text{ V}$. Overpotential (η) = 0 – E_{RHE} .

Femtosecond Transient Absorption Spectroscopy (fs-TAS) was performed on a pump–probe system (Helios, Ultrafast System) with the maximum time delay of ~8 ns using a motorized optical delay line under ambient conditions. The pump pulses at 350 nm (~20 μW average power at the sample) were delivered by an ultrafast optical parametric amplifier (OPera Solo) excited by a regenerative amplifier (Coherent Astrella, 800 nm, 35 fs, 5 mJ, 1 kHz), seeded with a mode-locked Ti:sapphire oscillator (Coherent Vitera, 800 nm, 80 MHz) and pumped with a LBO laser (Coherent Evolution-50C, 1 kHz system). A small amount of 800 nm femtosecond pulses from the regenerative amplifier were used to pump a sapphire crystal to create a 420–800 nm white light continuum as probe pulses. The

TA spectra were fitted with *Surface Explorer* software by the convoluted multi-exponential function:

$$\Delta A(t) = e^{-\left(\frac{t-t_0}{t_p}\right)^2} * \sum_{i=1}^N A_i e^{-\frac{t-t_0}{\tau_i}} \quad (1)$$

where t is the probe time delay, t_0 is time zero, $t_p = IRF/(2 \cdot \ln 2)$, IRF is the width of instrument response function (full width half maximum), A_i and τ_i are amplitudes and decay times, respectively, $*$ is convolution. The minimum number of components N to satisfactorily fit the experimental data is three.

1.4 Photocatalytic activity testing

The photocatalytic activity testing was performed in a 50 mL Quartz reactor. Typically, 15 mg of catalyst, 12 mM of nitrobenzene, 4 mL of 1,4-dioxane, 1 mL of ultrapure water and 0.5 mL of triethanolamine (TEOA) were added in the reactor. Then the reactor was sealed and purged with N_2 for 15 times by Multi-Atmosphere Controller (PLA MAC 1005, Beijing PerfectLight, China). Afterwards, the reactor was irradiated with an LED light (wavelength: 365 nm, PCX-50C Discover, Beijing PerfectLight, China) at 30 °C controlled by a DLSB (DL-400, Hangzhou Geng Yu Instrument Co., Ltd). The light intensity was 0.4 $W\ cm^{-2}$ measured by the radiant power energy meter (CEL-NP2000-2(10)A, Beijing China Education Au-light Co., Ltd). After reaction, the mixture was filtered to remove solid catalysts and then analyzed by a gas chromatograph (GC-2014C, Shimadzu Corp., Japan) equipped with a flame ionization detector (FID) and a capillary column (HP-5, 30 m \times 0.32 mm \times 0.25 μm , Agilent Technologies, USA). The column was maintained at 70 °C for 8

min, then heated to 250 °C at 40 °C min⁻¹ and maintained for another 2 min. The pressure of carrier gas was set to 80 kPa. The temperatures of the injector and the detector were set to be 250 and 270 °C, respectively. For reusability testing, the used catalysts were washed twice by ethanol, dried at 60 °C in a vacuum oven and reused in the next reaction cycle. The isotope labeling experiment was conducted by using D₂O (99.9%, Macklin) instead of ultrapure water as the hydrogen source. The protocol of photocatalytic activity testing was the same with that mentioned above. The products were analyzed by gas chromatography-mass spectrometry (TRACE 1300 and ISQ 7000, Thermo scientific, USA) equipped with the capillary column (HP-5, 30 m× 0.32 mm× 0.25 μm, Agilent Technologies, USA). Helium was the carrier gas with pressure set to 60 kPa. The temperatures of the injector, ion source and MS transfer line were set to be 250, 230 and 250 °C, respectively.

1.5 Computational details

The DFT calculations were carried out by using the Vienna Ab initio Simulation Package (VASP). The exchange–correlation interaction was described by generalized gradient approximation (GGA) with the Perdew–Burke–Ernzerhof (PBE) functional. The Brillouin zone was integrated with a Monkhorst – Pack 2×2×1 k-point grid and plane-wave energy cutoff of 520 eV for all calculations. Anatase (101)-(1×3), rutile (110)-(3×2) and Ce₂S₃ (001)-($\sqrt{2}\times\sqrt{2}$)R45° surfaces were built for adsorption energy calculations with DFT-D3 correction. A vacuum of 20 Å was used to eliminate interactions between periodic structures. Ce₂S₃ (001) surface was selected for simulation due to its lowest surface energy within the low-index facets (Table S1). The bottom half of atoms of the slab was fixed for

structural relaxation. The convergence criteria for energy and force were 10^{-5} eV and 0.02 eV/Å, respectively. All the parameters were optimized in terms of accuracy and computational time using results of preliminary calculations. The adsorption energy (E_{ads}) of adsorbate on TiO_2 or Ce_2S_3 surface slabs is defined as $E_{\text{ads}} = E_{\text{slab+adsorbate}} - E_{\text{slab}} - E_{\text{adsorbate}}$, where $E_{\text{slab+adsorbate}}$, E_{slab} and $E_{\text{adsorbate}}$ are the energies of surface slab with adsorbate, surface slab and adsorbate, respectively. The work function is defined as $\Phi = E_{\text{V}} - E_{\text{F}}$, where E_{V} and E_{F} are the electrostatic potentials of the vacuum and Fermi levels, respectively.

2. Supporting Figures

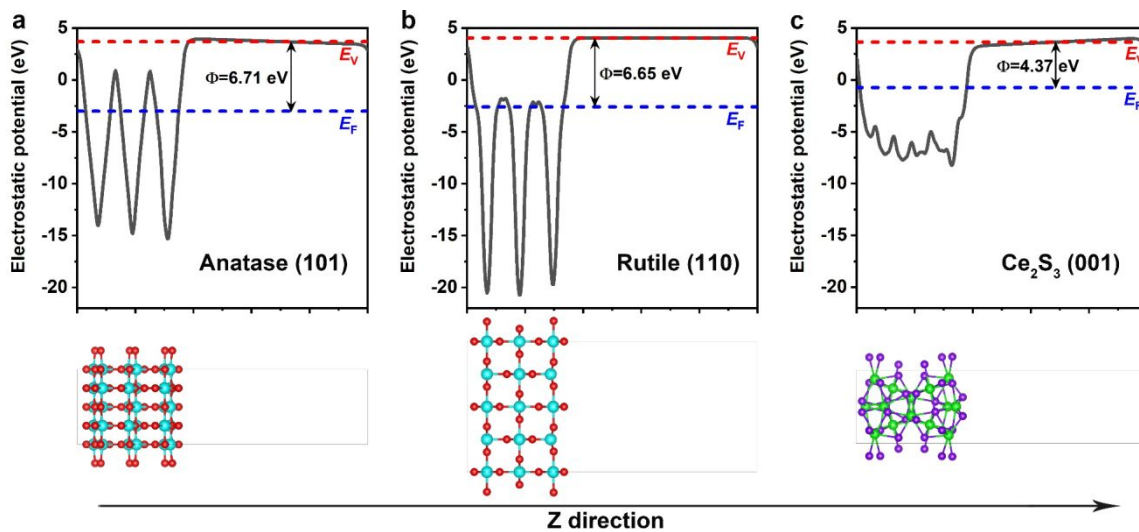


Figure S1. The calculation of work function. The electrostatic potentials of (a) anatase TiO_2 (101), (b) rutile TiO_2 (110) and (c) Ce_2S_3 (001) facets. The cyan, red, green and violet spheres stand for Ti, O, Ce and S atoms, respectively. Blue and red dashed lines indicate the Fermi and vacuum energy levels, respectively.

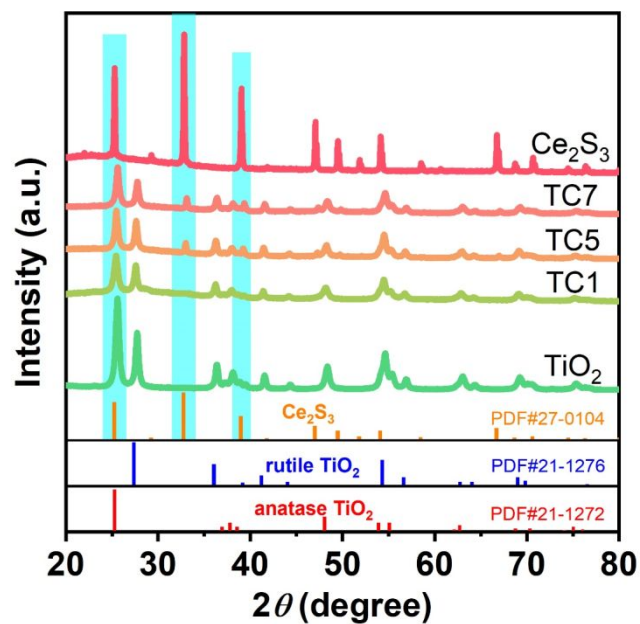


Figure S2. X-ray diffraction (XRD) patterns of TiO_2 , TC1, TC5, TC7 and Ce_2S_3 . TC x represents the $\text{TiO}_2/\text{Ce}_2\text{S}_3$ hybrids, where T and C represent TiO_2 nanofiber and Ce_2S_3 nanoparticle, respectively; x is the mole percentages of Ce_2S_3 with respect to TiO_2 .

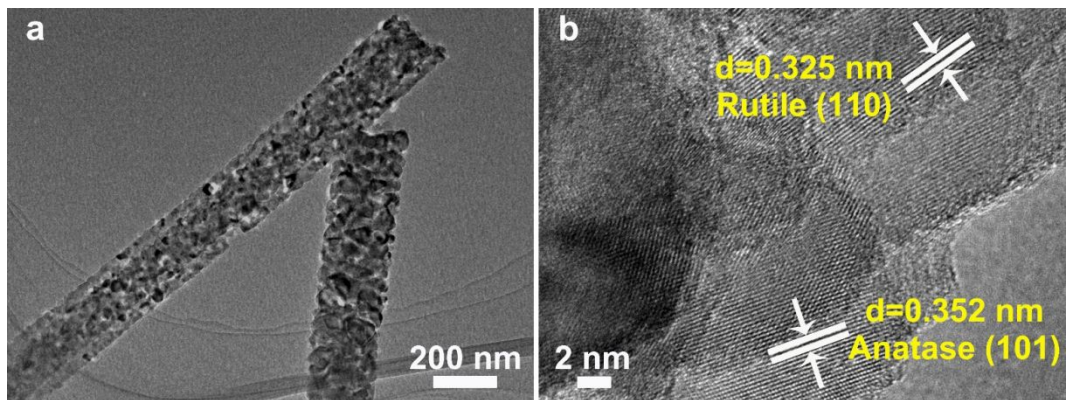


Figure S3. Morphology of TiO_2 nanofibers. (a) TEM image, (b) HRTEM image.

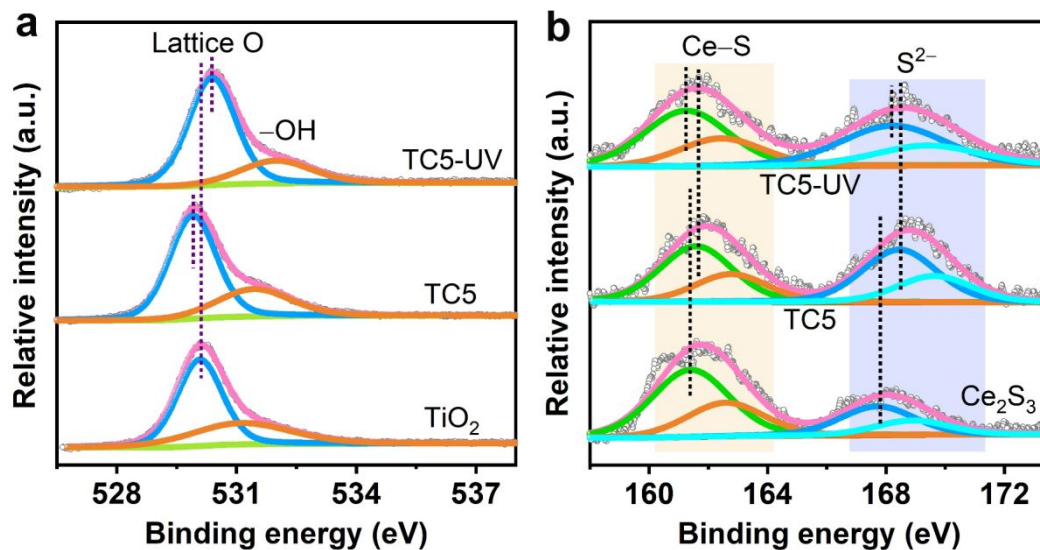


Figure S4. X-ray photoelectron spectroscopy (XPS) spectra of resultant samples. High resolution XPS spectra (a) O 1s of TiO₂ and TC5, (b) S 2p of Ce₂S₃ and TC5. *In-situ* XPS spectra were recorded under UV-vis light irradiation. TC5 represents the TiO₂/Ce₂S₃ hybrid, where T and C represent TiO₂ nanofiber and Ce₂S₃ nanoparticle, respectively; 5 is the mole percentages of Ce₂S₃ with respect to TiO₂.

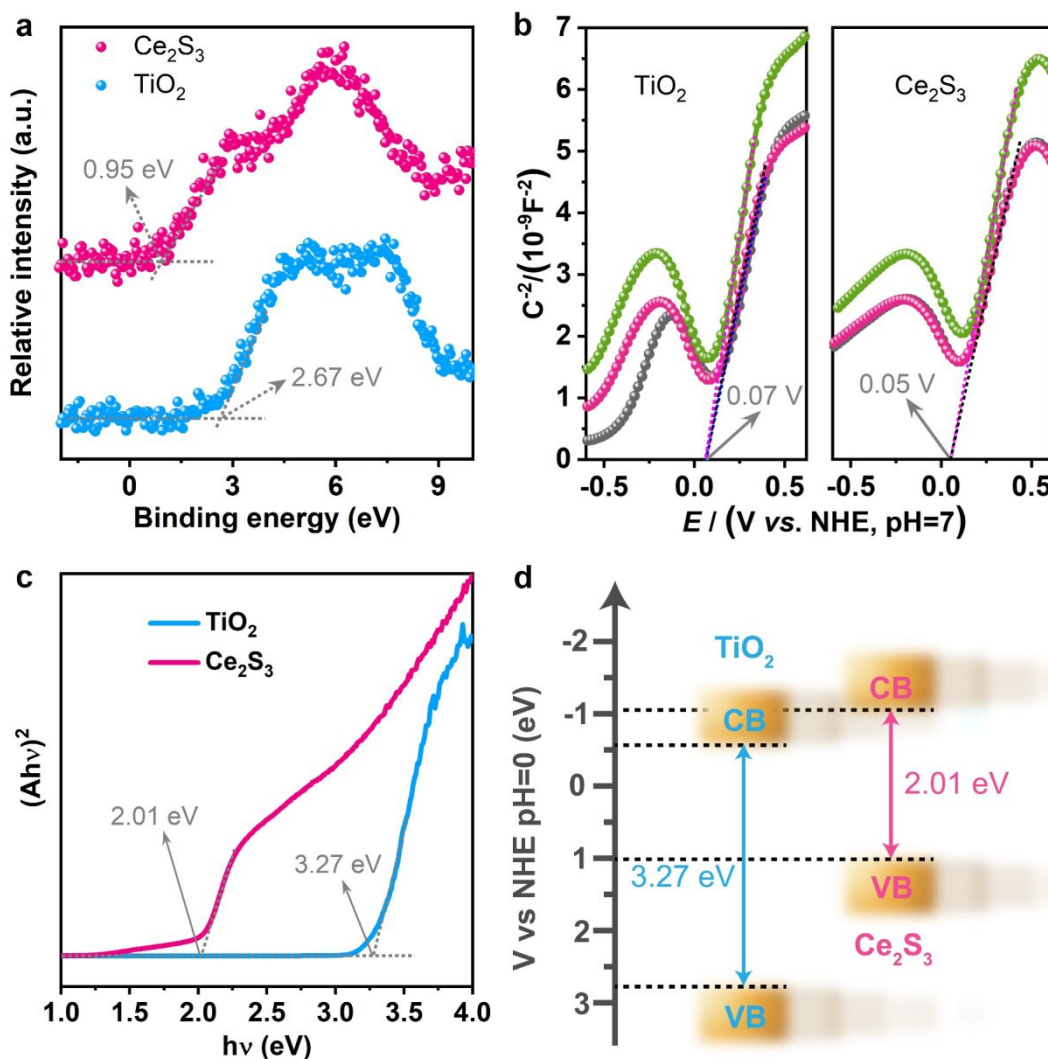


Figure S5. Band structures of TiO_2 and Ce_2S_3 . (a) Valence band (VB) XPS spectra, (b) Mott-Schottky plots and (c) Kubelka–Munk energy curve plots of TiO_2 and Ce_2S_3 . (d) Band structures of the composite photocatalyst.

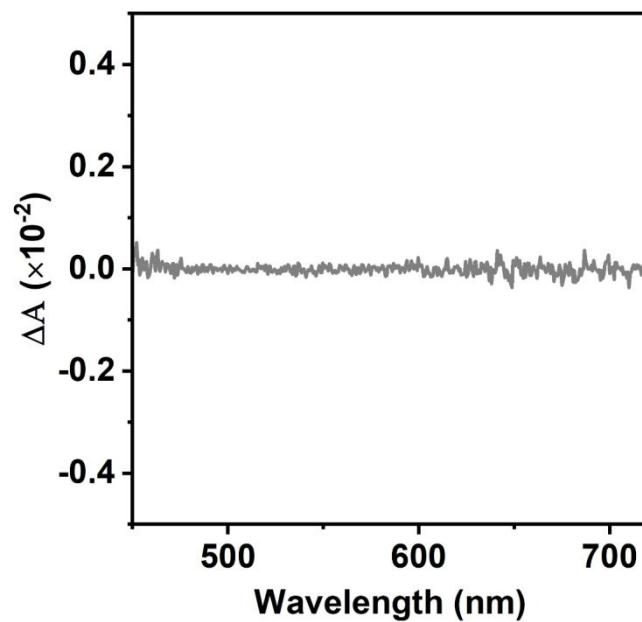


Figure S6. The transient absorption spectrum of TiO₂ nanofibers recorded following the addition of an electron scavenger (AgNO₃) and measured with 350 nm excitation.

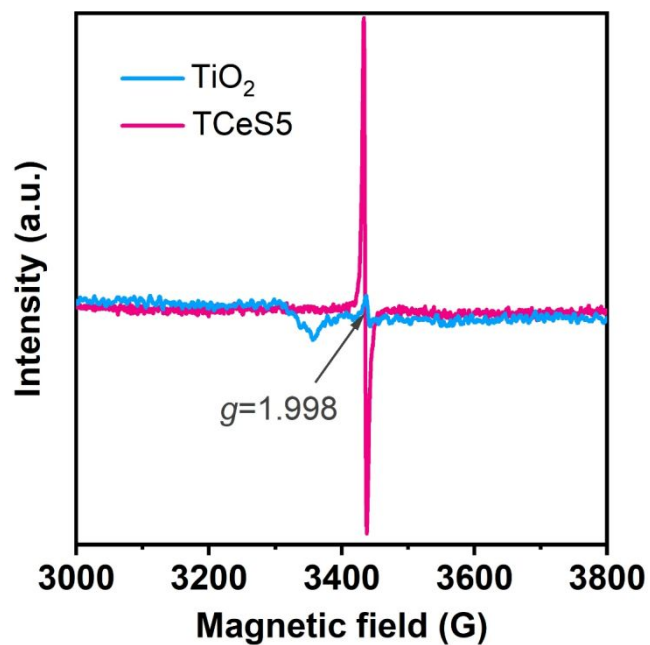


Figure S7. Electron spin resonance (ESR) spectra of TiO_2 and TC5. TC5 represents the $\text{TiO}_2/\text{Ce}_2\text{S}_3$ hybrids, where T and C represent TiO_2 nanofiber and Ce_2S_3 nanoparticle, respectively; 5 is the mole percentages of Ce_2S_3 with respect to TiO_2 .

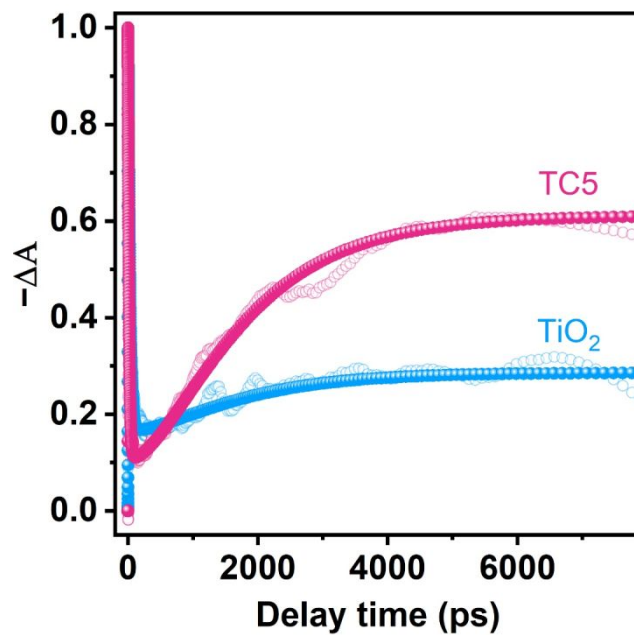


Figure S8. The transient absorption kinetic traces of TiO₂ and TC5 at 645 nm with prolonging the delay time.

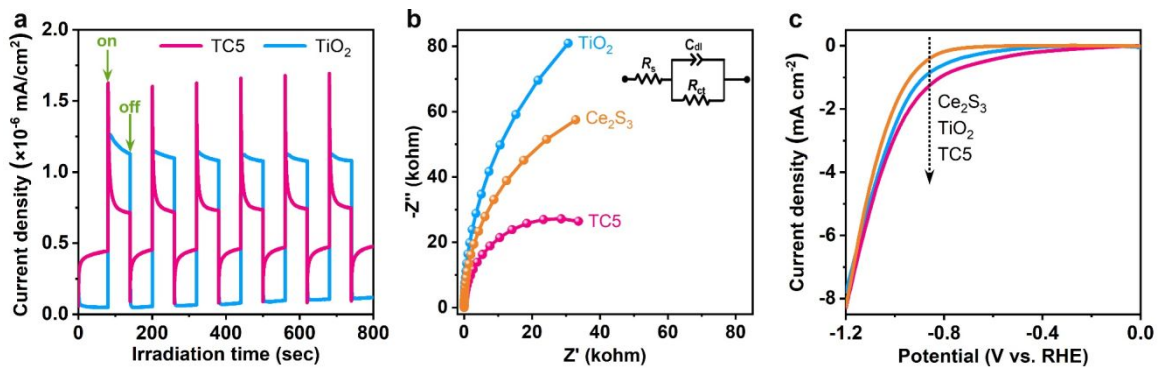


Figure S9. Electrochemical characterizations. (a) Transient photocurrent response for TiO₂ and TC5 under UV-visible light irradiation in 0.5 M Na₂SO₄ aqueous solution. (b) Nyquist plots of TiO₂, TC5 and Ce₂S₃ in 0.5 M Na₂SO₄ aqueous solution. (c) Polarization curves of TiO₂, TC5 and Ce₂S₃ at a scan rate of 5 mV s⁻¹ in 0.5 M Na₂SO₄ under UV-visible light irradiation. TC5 represents the TiO₂/Ce₂S₃ hybrids, where T and C represent TiO₂ nanofiber and Ce₂S₃ nanoparticle, respectively; 5 is the mole percentages of Ce₂S₃ with respect to TiO₂.

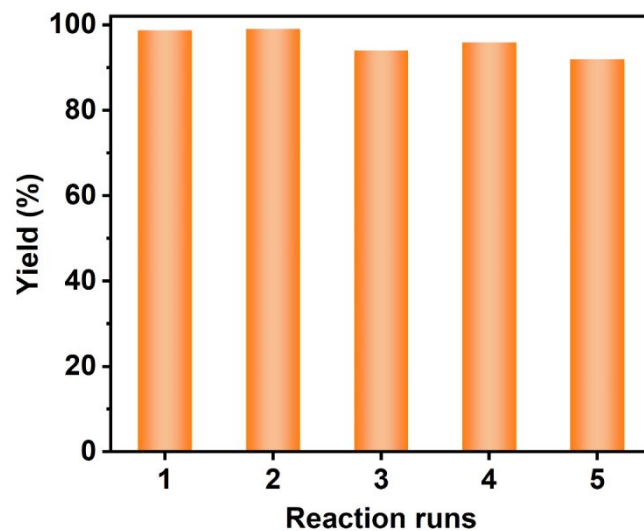


Figure S10. The recyclability of TC5 for the photocatalytic transfer hydrogenation. TC5 represents the $\text{TiO}_2/\text{Ce}_2\text{S}_3$ hybrid, where T and C represent TiO_2 nanofiber and Ce_2S_3 nanoparticle, respectively; 5 is the mole percentages of Ce_2S_3 with respect to TiO_2 .

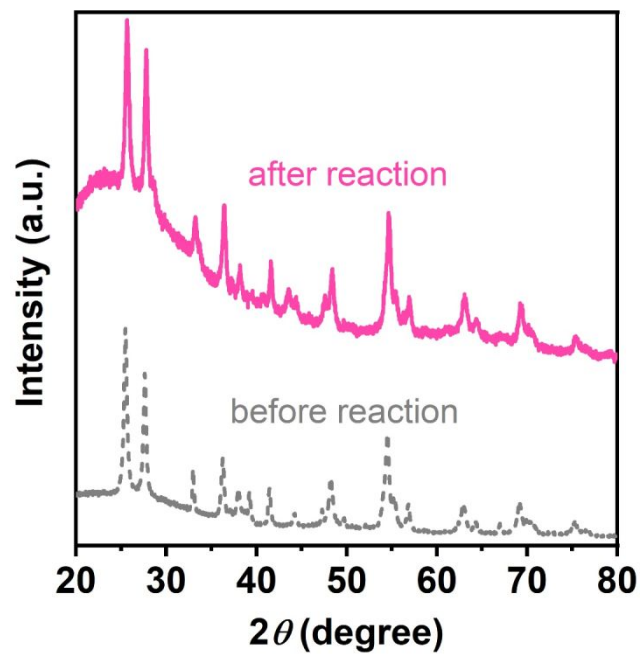


Figure S11. XRD patterns of TC5 before and after photocatalytic reaction. TC5 represents the $\text{TiO}_2/\text{Ce}_2\text{S}_3$ hybrid, where T and C represent TiO_2 nanofiber and Ce_2S_3 nanoparticle, respectively; 5 is the mole percentages of Ce_2S_3 with respect to TiO_2 .

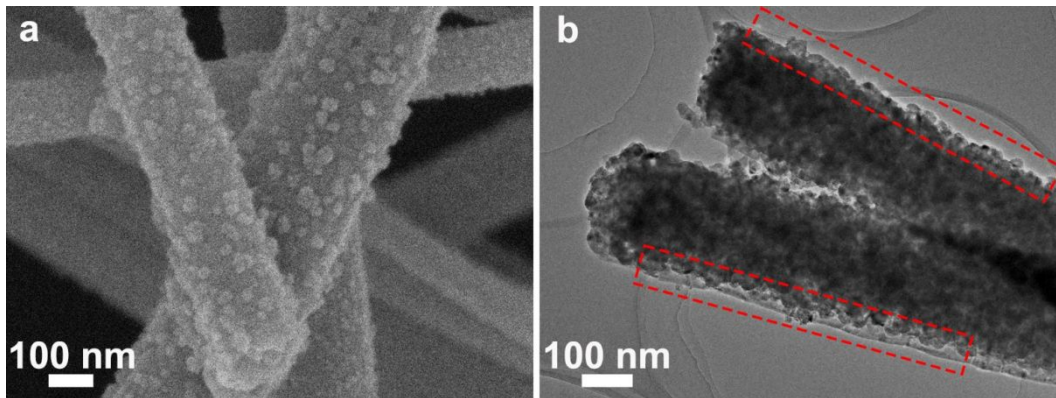


Figure S12. (a) FESEM and (b) TEM images of TC5 after photocatalytic reaction. TC5 represents the $\text{TiO}_2/\text{Ce}_2\text{S}_3$ hybrid, where T and C represent TiO_2 nanofiber and Ce_2S_3 nanoparticle, respectively; 5 is the mole percentages of Ce_2S_3 with respect to TiO_2 .

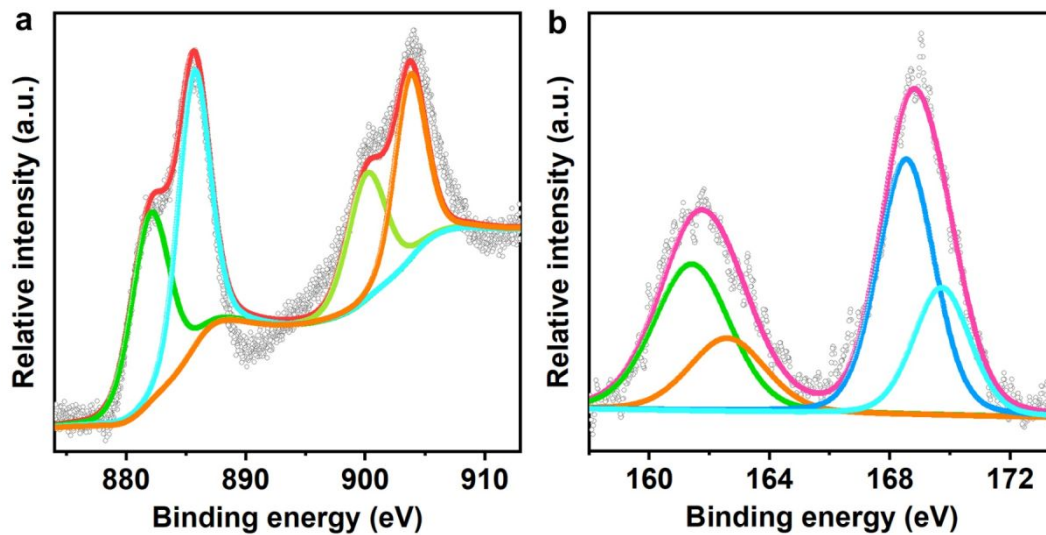


Figure S13. High resolution XPS spectra of (a) Ce 3d and (b) S 2p of TC5 after photocatalytic reaction. TC5 represents the $\text{TiO}_2/\text{Ce}_2\text{S}_3$ hybrid, where T and C represent TiO_2 nanofiber and Ce_2S_3 nanoparticle, respectively; 5 is the mole percentages of Ce_2S_3 with respect to TiO_2 .

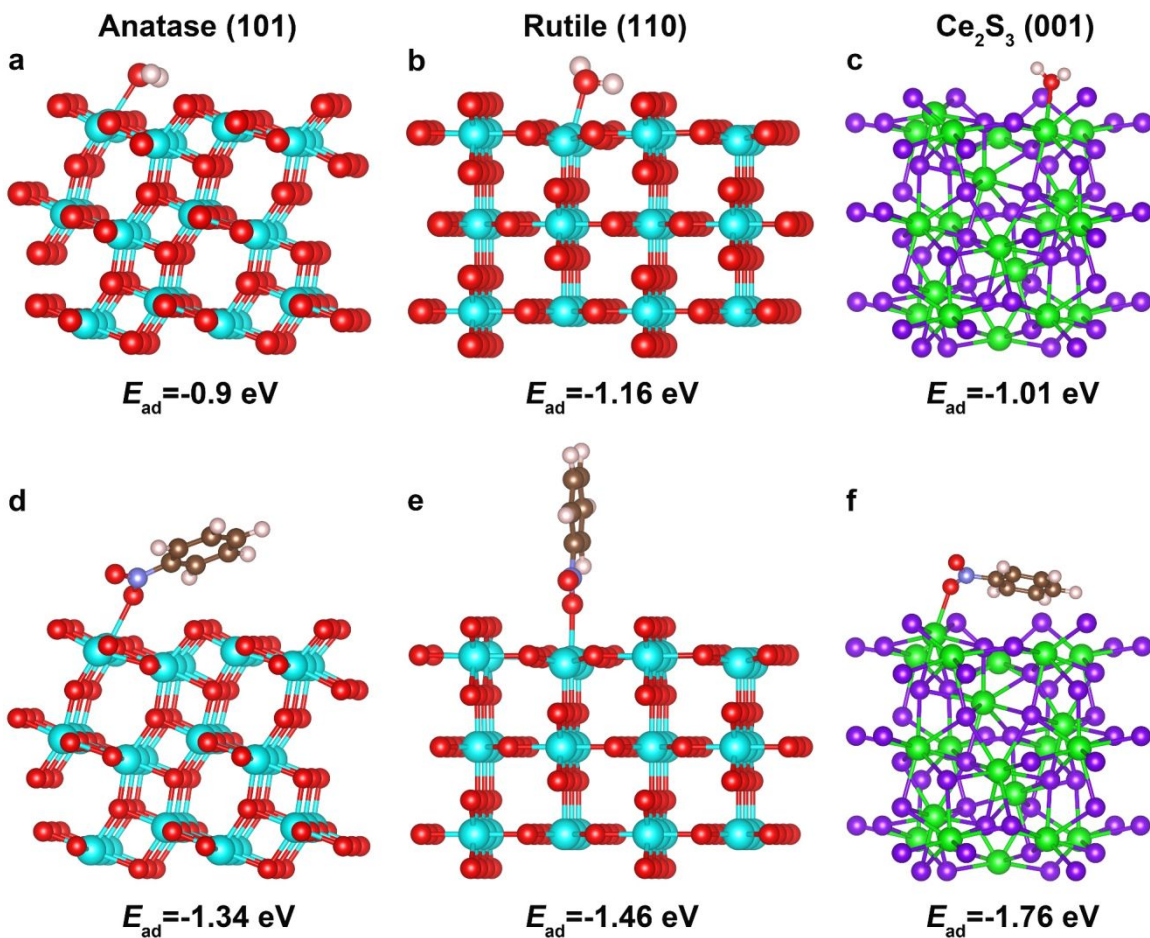


Figure S14. The adsorption of reactants. Optimized structures of H_2O and nitrobenzene molecules adsorbed on anatase TiO_2 (101), rutile TiO_2 (110), and Ce_2S_3 (001) facets. The cyan, red, green, violet, light pink, brown and blue spheres stand for Ti, O, Ce, S, H, C and N atoms, respectively.

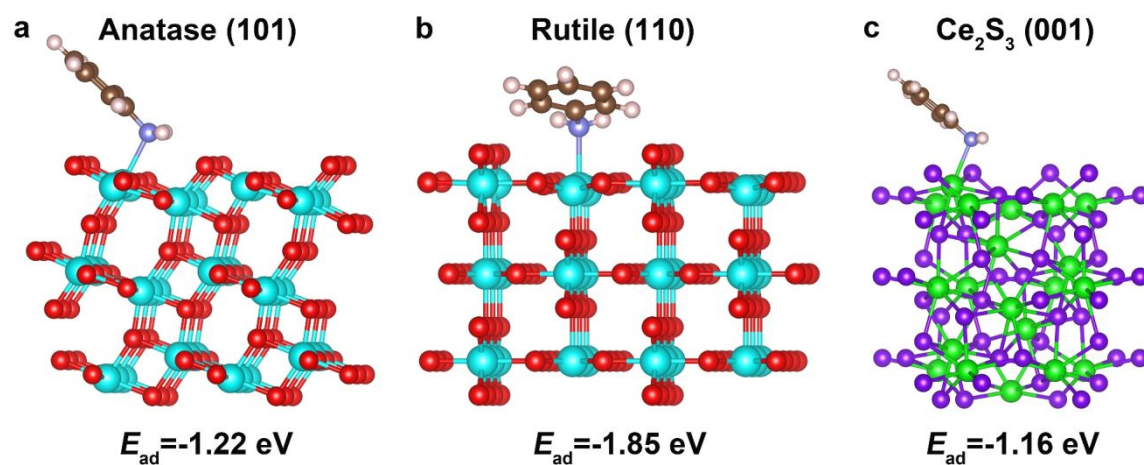


Figure S15. The desorption of products. Optimized structures of aniline molecule adsorbed on anatase TiO_2 (101), rutile TiO_2 (110), and Ce_2S_3 (001) facets. The cyan, red, green, violet, light pink, brown and blue spheres stand for Ti, O, Ce, S, H, C and N atoms, respectively.

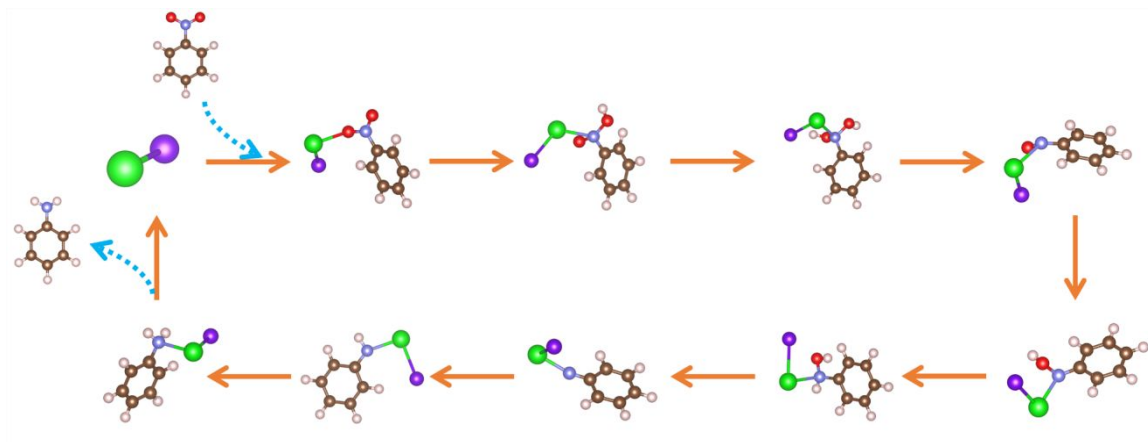


Figure S16. The photocatalytic hydrogenation process over $\text{TiO}_2/\text{Ce}_2\text{S}_3$ hybrid. The green, red, violet, light pink, brown and blue spheres stand for Ce, S, O, H, C and N atoms, respectively.

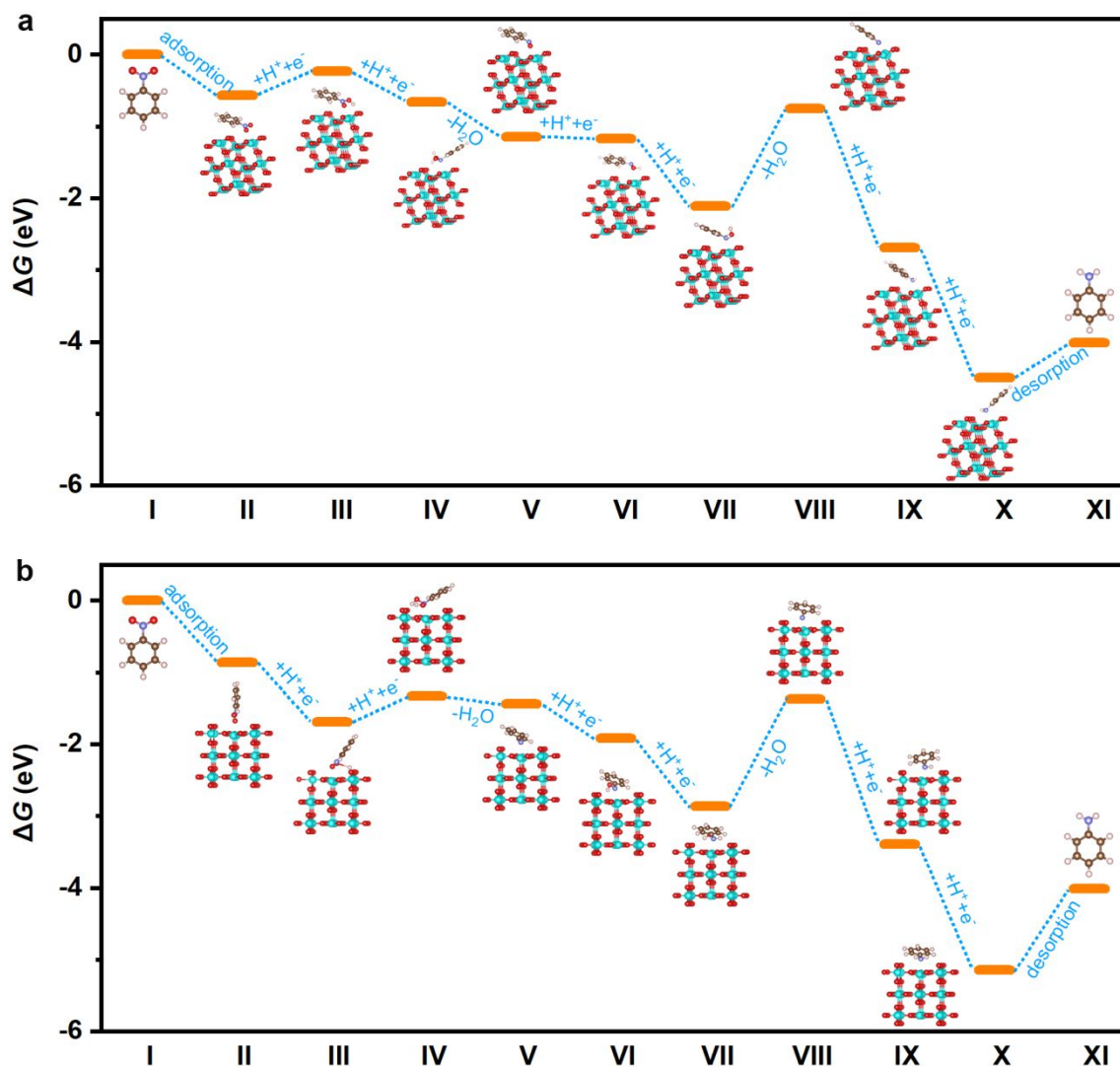


Figure S17. Free energy diagrams of photocatalytic nitrobenzene hydrogenation to aniline for: (a) anatase TiO_2 and (b) rutile TiO_2 single-unit-cell layers. The cyan, red, light pink, brown and blue spheres stand for Ti, O, H, C and N atoms, respectively.

3. Supporting Tables

Table S1. The calculated surface energy of the typical low-index surfaces of Ce₂S₃.

Facets	Surface energy (J m ⁻²)
(001)	0.34
(011)	0.59
(111)	0.80
(113)	0.73
(121)	0.91

The surface energy (σ) was given by the following equation:

$$\sigma = (E_{\text{slab}} - nE_{\text{bulk}})/2A$$

where E_{slab} is the total energy of the slab, E_{bulk} is the energy per atom of the bulk, n is the total number of atoms in the slab, and A is the surface area of the slab.

Table S2. Fitted electrochemical parameters of TiO₂, TC5 and Ce₂S₃ according to the equivalent circuit. TC5 represents the TiO₂/Ce₂S₃ hybrid, where T and C represent TiO₂ nanofiber and Ce₂S₃ nanoparticle, respectively; 5 is the mole percentages of Ce₂S₃ with respect to TiO₂.

Sample	R_s (Ω)	C (F)	R_{ct} (Ω)
TiO₂	21.6	1.45×10^{-5}	2.4×10^5
TC5	17.5	1.94×10^{-5}	5.4×10^4
Ce₂S₃	16.4	1.76×10^{-5}	1.3×10^5

R_s , C and R_{ct} represent the solution resistance, the capacitance and the charge transfer resistance, respectively.